



Published in final edited form as:

Epilepsia. 2014 December ; 55(12): 1986–1995. doi:10.1111/epi.12851.

The spatial and signal characteristics of physiologic high frequency oscillations

Rafeed Alkawadri*, Nicolas Gaspard*, Irina I. Goncharova*, Dennis D. Spencer†, Jason L. Gerrard†, Hitten Zaveri*, Robert B. Duckrow*†, Hal Blumenfeld*, and Lawrence J. Hirsch*

*Department of Neurology, Yale Comprehensive Epilepsy Center, New Haven, Connecticut, U.S.A

†Department of Neurosurgery, School of Medicine, Yale University, New Haven, Connecticut, U.S.A

Summary

Objectives—To study the incidence, spatial distribution, and signal characteristics of high frequency oscillations (HFOs) outside the epileptic network.

Methods—We included patients who underwent invasive evaluations at Yale Comprehensive Epilepsy Center from 2012 to 2013, had all major lobes sampled, and had localizable seizure onsets. Segments of non-rapid eye movement (NREM) sleep prior to the first seizure were analyzed. We implemented a semiautomated process to analyze oscillations with peak frequencies >80 Hz (ripples 80–250 Hz; fast ripples 250–500 Hz). A contact location was considered epileptic if it exhibited epileptiform discharges during the intracranial evaluation or was involved ictally within 5 s of seizure onset; otherwise it was considered nonepileptic.

Results—We analyzed recordings from 1,209 electrode contacts in seven patients. The nonepileptic contacts constituted 79.1% of the total number of contacts. Ripples constituted 99% of total detections. Eighty-two percent of all HFOs were seen in 45.2% of the nonepileptic contacts (82.1%, 47%, 34.6%, and 34% of the occipital, parietal, frontal, and temporal nonepileptic contacts, respectively). The following sublobes exhibited physiologic HFOs in all patients: Perirolandic, basal temporal, and occipital subregions. The ripples from nonepileptic sites had longer duration, higher amplitude, and lower peak frequency than ripples from epileptic sites. A high HFO rate (>1/min) was seen in 110 nonepileptic contacts, of which 68.2% were occipital. Fast ripples were less common, seen in nonepileptic parietooccipital regions only in two patients and in the epileptic mesial temporal structures.

Conclusions—There is consistent occurrence of physiologic HFOs over vast areas of the neocortex outside the epileptic network. HFOs from nonepileptic regions were seen in the occipital lobes and in the perirolandic region in all patients. Although duration of ripples and peak

Address correspondence to Rafeed Alkawadri, Comprehensive Epilepsy Center, Yale University, 15 York Street, LCI 7-14B, LLCI 7th floor, P.O. Box 208018, New Haven, CT, U.S.A. mhdrafeed.alkawadri@yale.edu.

Disclosure

Authors have nothing to disclose. We confirm that we have read the Journal's position on issues involved in ethical publication and affirm that this report is consistent with those guidelines.*

Supporting Information

Additional Supporting Information may be found in the online version of this article.

frequency of HFOs are the most effective measures in distinguishing pathologic from physiologic events, there was significant overlap between the two groups.

Keywords

High frequency oscillations; Intracranial EEG; Ripples; Epilepsy; Electrocorticography

Over the past few years, there has been growing interest in analysis of interictal high frequency oscillations (HFOs), primarily toward understanding their value for identifying the seizure-onset zone and their correlation with epileptogenicity. High-frequency oscillations (HFOs), namely ripples (80–250 Hz) and fast ripples (>250 Hz), have been recorded from the intracranial electroencephalography (icEEG) in patients with medically intractable focal epilepsy who were undergoing surgical evaluation.^{1–7} Some studies suggested that HFOs are more closely linked to the seizure-onset zone than interictal spikes.³ In addition, other studies suggested that removal of HFO-generating areas is associated with a favorable surgical outcome in children and adults with drug-resistant epilepsy.^{8,9} However, the reliability of HFOs as a biomarker of epileptogenicity and the seizure-onset zone remains uncertain.^{10,11} Lately, there has been a cumulative evidence suggesting that HFOs in general and ripples in particular are sometimes physiologic and not related to pathology in humans.^{4,10,12,13}

The primary goal of this study was to investigate the incidence, spatial distribution, and signal characteristics of spontaneous HFOs that occur outside the epileptic network in a group of patients with extensive spatial sampling.

Methods

Patients and EEG data acquisition

Patients with medically intractable epilepsy who underwent invasive icEEG evaluations at Yale Comprehensive Epilepsy Center between 2012 and 2013 were screened for inclusion in this study. Cases were included if (1) EEG was sampled at 1,024 Hz or higher, (2) all major lobes were sampled, and (3) EEG seizure onset was localizable.

Each subject underwent continuous icEEG recording with clinical video-EEG monitoring equipment. Subdural grids, multiple strips, and depth electrodes (AdTech Medical, Racine, WI, U.S.A.) were placed as required and discussed in a multidisciplinary surgical conference prior to implantation.

The subdural electrode contacts were 4 mm diameter platinum disks. The depth electrode contacts were 2.3 mm in length. Electrodes were placed with 10 mm center-to-center spacing. The icEEG was recorded on a commercially available 256–512 channel video-icEEG long-term monitoring system (5,000 Hz; Compumedics U.S.A. Inc., Charlotte, NC, U.S.A. or 1,024 Hz; Natus Medical Inc, San Carlos, CA, U.S.A.). The recordings were referenced to an electrode implanted within the diploic space. HFO analysis was performed using a referential montage.

Detection of high frequency oscillations

Two 10-min segments of slow wave sleep, one and two nights prior to recording of the first seizure were identified for analysis.^{3,14}

Each record was visually screened for qualitative HFO analysis. Each channel was classified in one of four categories according to HFOs rate (absent; rare, 1–10/10 min; very frequent, >10/min; or frequent, between rare and very frequent). This step was undertaken prior to the automatic analysis, and the results were recorded independent of the automatic detection. The purpose of this step is to adjust the automatic threshold to account for channels with high rates of HFOs, which prompted lowering the threshold to ensure detection of all channels that exhibited HFOs at rates consistent with qualitative rates identified visually.

We used a custom-developed semiautomated MATLAB program (The Math Works, Inc., Natick, MA, U.S.A.) to detect and analyze oscillations with peak frequencies >80 Hz. The analysis was implemented using a two-step approach. The first step was automatic, and based on previously described detector using root mean square (RMS) power.^{15,16} In the second step, an expert human-reader flagged detections for inclusion or rejection. The visual analysis of HFOs was done as detailed below.³

Detection and verification

Each channel of icEEG data was digitally filtered with a band-pass of 80 and 500 Hz for ripple analysis, and 250 and 500 Hz for fast ripple analysis. We employed a fourth-order Butterworth band-pass filter.

Ripples—The RMS of a sliding window (N) = 30 msec, and a step (dt) = 1 msec, was calculated on the filtered signal for the entire time-series.

$$\text{RMS}(t) = \sqrt{\frac{1}{N} \sum_{k=t-N+1}^t x^2(k)}$$

Because the data set of RMS values is not normally distributed, we selected a nonparametric global threshold by examining the global empirical cumulative distribution of RMS values from all channels in relation to a 3-min baseline.

The first tested percentile was 97.5. The global threshold was subsequently lowered by 2.5 percentile steps (e.g., 97.5 to 95 to 92.5) until each channel that exhibited at least one HFO event was detected at rates that met or exceeded the visual screening. The range of the final threshold was 80–85, depending on the total number of detections. This is a more inclusive threshold compared to thresholds commonly implemented.¹⁵ The second step of the analysis, which was expert guided, aimed to verify detections and exclude false ones.

The following values were saved for each detection: Time of detection, peak-to-peak amplitude, duration, and peak frequency. We used a Welch's averaging estimator on a 32 msec window centered on the HFO to estimate the peak frequency (16 msec for fast ripples). Each automatic detection was reviewed by an expert using a graphical user interface, which

contained a 2 s epoch of the raw data, and 1 s and 2 s epochs of the filtered data. A candidate HFO event was accepted if (1) it contained at least four consecutive oscillations, (2) its amplitude was at least two times higher than non-HFO background, and (3) the oscillations could be discerned on the unprocessed icEEG signal. The last step ensured that oscillations introduced by filtering were excluded.¹⁷

Fast ripples—To address important methodologic pitfalls that were discussed in a previous study,¹⁷ we used four windows, all 250 msec long in duration (RMS window 10 msec); one contained unprocessed EEG data, two contained processed data with band-pass filters of (80 and 250–500), and the last window was a Morlet wavelet–based spectral density plot normalized to the maximum power in 250–500 range. The spectral analysis was implemented to exclude artifacts due to harmonics of spikes and ripples.¹⁷ In addition to the inclusion criteria implemented in ripple analysis, a fast ripple event was marked for inclusion only if its waveforms were visible on the window with high-pass filter of 80 Hz prior to filtering, and it occupied a distinct “blob” in the spectral density plots.¹⁷ This led to inclusion of only a small fraction of the automatic fast ripple detections (0–11% per case at 97.5 percentile). (See Figure S1 for examples of detections and extracted parameters.)

The beginning and the end of each HFO event were manually marked to estimate the event’s duration and amplitude. We used the oscillations on the unprocessed data to determine the onset and offset of an event. The amplitude of an event was measured between the maximum negative and positive peaks on a referential montage.

Classification of the electrode contacts

For the purposes of this study, a contact location was classified as epileptic if (1) it exhibited epileptiform discharges during the interictal period, or (2) it was involved in the seizure within 5 seconds^{18,19} of EEG seizure onset.^{20,21} A contact location was otherwise classified as nonepileptic.

Coregistration of the contacts with preoperative MRI, and visualization of HFOs

We used preimplantation, postimplantation magnetic resonance imaging (MRI) studies, and postimplantation computerized tomography (CT) scan to perform this step. Each electrode contact was coregistered with a preimplantation three-dimensional triangular mesh model of each patient’s cortex using the coregistration tools available in BioImage Suite software (v3.0; New Haven, CT, U.S.A.). Each contact was assigned a lobe (frontal, parietal, temporal, occipital, and insular) and a sublobe (lateral frontal, medial frontal, orbitofrontal, medial parietal, lateral parietal, lateral temporal, mesial temporal, basal temporal, lateral occipital, medial occipital, and basal occipital) based on its spatial relationship to anatomic landmarks. (See Fig. 1) for summary of distribution of included contacts and their classification. To visualize HFO data from all patients in a common space, electrode contact locations were transformed into a standardized space using a nonlinear coregistration of a standard brain (Montreal Neurological Institute [MNI] brain). For details of the transformation, refer to BioImage Suite manual available at (<http://medicine.yale.edu/bioimaging/suite/>). For realistic visualization of the spatial distribution and rate of the HFOs, we constrained visualization of HFOs to a mesh of the cortex (Mesh and brain template

available in Brainstorm [<http://neuroimage.usc.edu/brainstorm>]. We used nearest neighbor linear interpolation to 100 vertices around the center of each electrode contact.

Statistical analysis

The primary parameters tested across groups were amplitude, duration, and peak frequency of HFO events. These values were compared for significant differences between pathologic and nonepileptic sites, and among major lobes. We used nonparametric methods of analysis, namely Wilcoxon signed-rank test for paired comparisons, Mann-Whitney *U* test for unpaired comparisons, and Kruskal-Wallis for multiple group comparisons. Our accepted pretest probability of error (p-value) was <0.05. The comparisons were performed on a subset of detections normalized by patient and lobe. The subset consisted of 10 randomly selected nonepileptic HFO events from each major lobe and patient, thus 40 nonepileptic HFO events per patient, as well as randomly selected 40 epileptic HFOs per patient. The comparisons were performed on the entire cohort of detections as well. Receiver operating characteristic (ROC) curves were calculated to estimate the effective cutoff for each parameter to differentiate between epileptic and physiologic HFOs. Statistical testing for significance was performed using JMP (version 9; SAS Institute Inc., Cary, NC, U.S.A.).

Results

See Table 1 for summary of clinical data. Seven patients were included; four were female. The median age at time of epilepsy onset was 11 years (range 5–28 years). The median number of contacts was 175 (range 117–220 contacts/patient).

A total of 1,209 contacts were included in the analysis. (See Fig. 2 for details on localization and classification of all electrode contacts.) The sampled cortical regions spanned areas in both hemispheres in five patients. The frontal, temporal, parietal, occipital, and insular regions contained 498, 364, 182, 159, and 6 contacts constituting 41%, 30%, 15%, 13%, and <1% of the electrode contacts, respectively. Of the 1,209 electrode contacts, 958 were classified as nonepileptic (79.3%). The seizure onset was temporal in five (two mesial temporal, three neocortical), orbitofrontal-temporal in one patient, and temporoparietal in another patient. Ripples constituted 99% of detections in both epileptic and nonepileptic regions. They were seen consistently and frequently in all patients. In contrast, fast ripples were rare events and seen less consistently (1%) of all detections. HFOs from nonepileptic sites constituted 82.4% of total (21,214) events detected, and were seen in all major lobes in all patients. Nonepileptic HFOs were seen at least once in 429 electrode contacts, constituting 44.8% of the nonepileptic contacts (82.1%, 47%, 34.6%, and 34% of the occipital, parietal, frontal, and temporal nonepileptic contacts, respectively). The following sublobes were consistently involved: lateral frontal, lateral parietal, all occipital subregions, basal temporal, and orbitofrontal (See Figures 1 and 2).

Channels with the highest rate of HFOs were in the occipital lobes in all patients. The extraoccipital contact with highest nonepileptic HFO rate was seen in the functional hand motor area as delineated by electrical cortical stimulation in three of three patients where cortical stimulation was performed and in the expected anatomic hand motor area in six of six patients in whom anatomic hand motor areas were sampled (see Fig. 1).

High discharge rate (>1 HFO event per min per contact, ripples only) was seen in 110 nonepileptic electrode contacts (11.5% of nonepileptic contacts), of which 68.2% were located in the occipital region (and were found in all patients, that is, at least one contact in every patient), 16.5% frontal, 10% parietal, and 5.5% temporal regions. This represents 47.3%, 2.3%, 5.4%, and 3.9%, respectively, of the total number of the nonepileptic contacts within those regions. High discharge rate was seen in 34 epileptic contacts (13.5% of the epileptic contacts, primarily ripples), of which 70%, 18%, and 12% were located in the temporal, frontal, and occipital regions, respectively. This represents 10.4%, 28.6%, and 44%, respectively, of the epileptic contacts in those regions.

See Figure 3 for histograms of all ripple detections according to amplitude, duration, peak frequency, and rate. The ripples from nonepileptic sites exhibited longer duration (median 173 vs. 126 msec, $p < 0.0001$), higher amplitude (median 56 vs. 50 μV , $p = 0.001$), and lower median peak frequency (median 100 vs. 102 Hz, $p = 0.046$), after we controlled for the number of ripple events per lobe and patient. Similar trend was observed when the comparisons were performed for each lobe, with even lower p-values, with the exception of the parietal lobe where the number of pathologic detections was relatively low in this cohort.

Nonepileptic ripples in the occipital lobe were statistically longer in duration, higher in amplitude, and had a higher peak frequency than other lobes. Similar trends were seen within other lobes as well (Fig. S2).

Although the most distinguishing feature of nonepileptic ripples from epileptic ripples was duration both by statistical significance and absolute values, the overlap between the pathologic and physiologic ripples was extensive, and the most effective cutoffs (168 msec for HFO events and 242 msec for maximum duration per HFO-positive channel) resulted in only a modest sensitivity and specificity (See Fig. 4 for details.)

Ripple oscillations with peak frequencies higher than 150 Hz were seen primarily (>99.6%) at epileptic sites or in the occipital regions. The peak frequency was <128 Hz in 91% of the detections from nonepileptic sites (Fig. 3). The sensitivity, specificity, positive predictive, and negative predictive values of a contact with ripples for the seizure onset zone were 85.1%, 54.3%, 4%, and 99.3% respectively.

Fast ripples

A total of 278 fast ripple events in 19 contacts were detected. Of those, 110 events were recorded in 9 nonepileptic contacts. All 19 contacts were ripple positive. The nonepileptic contacts with fast ripples were located in the parietooccipital region (seven contacts), and the lateral perirolandic region (two contacts) in two patients. Fast ripples were found at highest rate in the epileptic mesial temporal structures (up to four per minute) in three of four patients with sampling from pathologic hippocampi. In one patient, they were found in the basal temporal epileptic area (four contacts) and in the same patient over restricted areas of epileptic neocortex (two contacts). There was a trend for higher peak frequency at the epileptic sites (medians 322 Hz vs. 272 Hz, $p = 0.1$). The duration and amplitude were not statistically different (median amplitudes 19 and 17 μV , median duration 24 and 19 msec for nonepileptic and pathologic fast ripples, respectively). The sensitivity, specificity, positive

predictive, and negative predictive values of a contact with fast ripples for early seizure involvement were 13.1%, 98.2%, 52.6%, and 95.7%, respectively.

Discussion

This study illustrates the frequent, consistent, and symmetric occurrence of nonepileptic ripples over vast areas of the neocortex during sleep in all the subjects, and the abundant occurrence over certain regions, primarily the occipital and perirolandic areas. In this cohort of patients with extensive spatial sampling, it was more likely for a ripple event to arise from nonepileptic sites than from epileptic sites (normalized ratio of 1.3 for individual HFO event). Ripples were seen in all the major regions of the brain in all patients. The following regions exhibited HFOs most consistently: Lateral frontal, lateral parietal, basal temporal, and all occipital subregions. Ripples were also seen in orbitofrontal and frontopolar areas. The insular region was not involved when sampled. Fast ripples were rare; they were infrequently found over restricted areas of the nonepileptic parietooccipital and lateral frontal cortices in two patients at significantly lower rates than ripples. Fast ripples were found at higher rates in the epileptic mesial temporal structures.

We believe that the nonepileptic HFOs in our cohort are a product of a physiologic rather than pathologic process for the following reasons: (1) the consistent and symmetric occurrence in certain regions in all patients, and within the same patient in the case of bilateral sampling; (2) the statistically significant differences in signal parameters between the two groups; and (3) the overlap and vicinity to the anatomic primary visual (most consistently), motor, and premotor areas as shown in this study and others.^{23–28}

The physiologic HFOs occurred at the highest rate in the occipital regions, followed by the hand motor area. Nonepileptic ripples are longer in duration, higher in amplitude, and have lower peak frequency than epileptic ripples. The difference in duration appears to be the most distinguishing feature, both by absolute values and statistical significance. Nevertheless, none of the cutoffs of the signal parameters was both highly sensitive and specific for reliable distinction. Based on ROC curves, the proposed duration cutoffs are 168 msec for HFO events and 242 msec for maximum duration per channel. In addition, channels that exhibited ripples with peak frequency higher than 185 Hz and fast ripples were fairly specific for pathology; however, this measure was not sensitive. Despite their specificity, fast ripples achieved only modest positive predictive values owing to the extensive spatial sampling that allowed detections outside the epileptic networks. Our findings are in agreement with the recent proposal²² that HFOs lasting >500 msec are more likely to arise from nonepileptic sites (91% of the channels that met this criterion in this cohort). However it differs in that sporadic ripple activity <200 msec in duration was not highly predictive of pathologic sites in this cohort (only 41% of the contact sites that met this definition were pathologic). The nonepileptic contacts that exhibited short-duration ripples were consistently located in the orbitofrontal, lateral frontal, and parietotemporal, and temporooccipital junctions.

In our study, the relative lower predictive value of an HFO event as a marker of pathology supports the observation¹⁰ that analysis of interictal HFOs is more reliable when it is

coupled with the analysis of other markers of the irritative zone such as spikes, or perhaps during active seizures.^{29–31} There was discrepancy between the sensitivity of ripples and specificity of fast ripples on one hand, and the low predictive values of HFOs as a marker of pathology. We attribute this discrepancy to the abundance of ripples in nonepileptic sites (i.e., “false positives”), and the relatively low ratio of pathologic to nonepileptic contacts (i.e., “prevalence”). In the case of fast ripples, the extensive spatial sampling allowed for detections outside the epileptic network accounting for the modest positive predictive values despite the high specificity. Our findings emphasize the importance of careful interpretation of HFOs, especially in cases with extensive spatial sampling, or when there is an overlap between the epileptic areas and one of the active physiologic areas identified in our study. There are currently no established criteria for distinguishing physiologic from pathologic HFOs,^{4,32} and using one parameter such as frequency or duration alone is not adequate³³ as illustrated in this study. The rarity of fast ripples in this cohort is consistent with some reports.¹⁰ In addition, there have been reports of low rates of fast ripples or no detection of fast ripples in the literature.^{7,34,35}

We speculate that some of the differences between our findings and some of the available literature stem from the extent of spatial sampling, methods undertaken to exclude detections with filtering artifact especially in the fast-ripple band, review montage (referential vs. bipolar),³⁶ methods implemented in the analysis (energy-based fully automatic vs. manual), frequency estimator (peak to peak duration vs. fixed-window-spectral-based), areas sampled, amplitude criteria, size of contacts, and time of analysis and relation to tasks among others. These factors may be taken into account when comparing results of different studies.

Limitations and Future Directions

Currently there is no available biomarker of the epileptogenic zone to reliably identify relevant pathologic tissue. Thus, in a cohort composed of patients with epilepsy, it is difficult to examine where a contact location resides on the broad spectrum between normality and pathology. In this study, we used the seizure-onset zone, propagation zone, and the irritative zone coupled with good surgical outcomes as biomarkers of pathology. Although this approach is commonly employed, we acknowledge that this concept is simplistic and has inherent limitations. However, the consistent and symmetric occurrence of HFOs across all subjects strongly supports the hypothesis that recorded HFOs are indeed physiologic. Access to certain regions such as the cingulate cortex was limited. Therefore, we are not able report on the occurrence of physiologic events in that region.

Future studies may explore the potential role of HFOs in task-free identification of physiologic brain networks. More than 91% of the physiologic HFOs exhibited peak frequencies <128 Hz, suggesting that it is possible to study this subgroup of oscillations with lower sampling rates than commonly employed, thus facilitating the inclusion of a larger number of cases using more conventional sampling rates. In addition, future studies may explore the electrographic behavior of areas known to generate physiologic HFOs when it overlaps with epileptic network.

Conclusions

In patients with extensive hemispheric coverage, ripples are seen consistently and symmetrically over vast areas of the neocortex outside the epileptic network and are abundant in certain brain regions such as the occipital and perirolandic areas. This study highlights the importance of establishing methods to distinguish pathologic HFOs from physiologic HFOs to further their use in clinical epileptology. Although duration and peak frequency are the most effective distinguishing features, there was extensive overlap between the groups. Fast ripples are rare events. They can be detected outside the epileptic network as well. Their predictive values may become diluted in cases with extensive spatial sampling especially in extratemporal regions. The results of our study emphasize the importance of careful interpretation of HFO analysis, especially in cases with extensive spatial sampling, or when the epileptic areas overlap with the active physiologic areas delineated in our study.

Supplementary Material

Refer to Web version on PubMed Central for supplementary material.

Acknowledgments

We wish to acknowledge the generous support of the Swebilius trust. We thank Mrs. Rebecca Khozein DOM, MS, REEG/EPT, RPSGT, RNCST, and Tamara Wing R.EEG T for their help with EEG data acquisition. We thank Norman So M.D. for his comments.

Biography



Rafeed Alkawadri is an attending Epileptologist at the Yale Comprehensive Epilepsy Center.

References

1. Bragin A, Engel J Jr, Wilson CL, et al. Hippocampal and entorhinal cortex high-frequency oscillations (100–500 Hz) in human epileptic brain and in kainic acid–treated rats with chronic seizures. *Epilepsia*. 1999; 40:127–137. [PubMed: 9952257]
2. Tatum WO, Dworetzky BA, Freeman WD, et al. Artifact: recording EEG in special care units. *J Clin Neurophysiol*. 2011; 28:264–277. [PubMed: 21633252]
3. Jacobs J, LeVan P, Chander R, et al. Interictal high-frequency oscillations (80–500 Hz) are an indicator of seizure onset areas independent of spikes in the human epileptic brain. *Epilepsia*. 2008; 49:1893–1907. [PubMed: 18479382]
4. Engel J Jr, Bragin A, Staba R, et al. High-frequency oscillations: what is normal and what is not? *Epilepsia*. 2009; 50:598–604. [PubMed: 19055491]

5. Jacobs J, Levan P, Chatillon CE, et al. High frequency oscillations in intracranial EEGs mark epileptogenicity rather than lesion type. *Brain*. 2009; 132:1022–1037. [PubMed: 19297507]
6. Jacobs J, Zelmann R, Jirsch J, et al. High frequency oscillations (80–500 Hz) in the preictal period in patients with focal seizures. *Epilepsia*. 2009; 50:1780–1792. [PubMed: 19400871]
7. Crepon B, Navarro V, Hasboun D, et al. Mapping interictal oscillations greater than 200 Hz recorded with intracranial macroelectrodes in human epilepsy. *Brain*. 2010; 133:33–45. [PubMed: 19920064]
8. Jacobs J, Zijlmans M, Zelmann R, et al. High-frequency electroencephalographic oscillations correlate with outcome of epilepsy surgery. *Ann Neurol*. 2010; 67:209–220. [PubMed: 20225281]
9. Akiyama T, McCoy B, Go CY, et al. Focal resection of fast ripples on extraoperative intracranial EEG improves seizure outcome in pediatric epilepsy. *Epilepsia*. 2011; 52:1802–1811. [PubMed: 21801168]
10. Wang S, Wang IZ, Bulacio JC, et al. Ripple classification helps to localize the seizure-onset zone in neocortical epilepsy. *Epilepsia*. 2013; 54:370–376. [PubMed: 23106394]
11. Haegelen C, Perucca P, Chatillon CE, et al. High-frequency oscillations, extent of surgical resection, and surgical outcome in drug-resistant focal epilepsy. *Epilepsia*. 2013; 54:848–857. [PubMed: 23294353]
12. Nagasawa T, Juhasz C, Rothermel R, et al. Spontaneous and visually driven high-frequency oscillations in the occipital cortex: intracranial recording in epileptic patients. *Hum Brain Mapp*. 2012; 33:569–583. [PubMed: 21432945]
13. Restuccia D, Del Piero I, Martucci L, et al. High-frequency oscillations after median-nerve stimulation do not undergo habituation: a new insight on their functional meaning? *Clin Neurophysiol*. 2011; 122:148–152. [PubMed: 20619726]
14. Staba RJ, Bergmann PC, Barth DS. Dissociation of slow waves and fast oscillations above 200 Hz during GABA application in rat somatosensory cortex. *J Physiol*. 2004; 561:205–214. [PubMed: 15550468]
15. Gardner AB, Worrell GA, Marsh E, et al. Human and automated detection of high-frequency oscillations in clinical intracranial EEG recordings. *Clin Neurophysiol*. 2007; 118:1134–1143. [PubMed: 17382583]
16. Staba RJ, Wilson CL, Bragin A, et al. Quantitative analysis of high-frequency oscillations (80–500 Hz) recorded in human epileptic hippocampus and entorhinal cortex. *J Neurophysiol*. 2002; 88:1743–1752. [PubMed: 12364503]
17. Benar CG, Chauviere L, Bartolomei F, et al. Pitfalls of high-pass filtering for detecting epileptic oscillations: a technical note on “false” ripples. *Clin Neurophysiol*. 2010; 121:301–310. [PubMed: 19955019]
18. Kim DW, Kim HK, Lee SK, et al. Extent of neocortical resection and surgical outcome of epilepsy: intracranial EEG analysis. *Epilepsia*. 2010; 51:1010–1017. [PubMed: 20384767]
19. Bartolomei F, Chauvel P, Wendling F. Epileptogenicity of brain structures in human temporal lobe epilepsy: a quantified study from intracerebral EEG. *Brain*. 2008; 131:1818–1830. [PubMed: 18556663]
20. Nair DR, Burgess R, McIntyre CC, et al. Chronic subdural electrodes in the management of epilepsy. *Clin Neurophysiol*. 2008; 119:11–28. [PubMed: 18035590]
21. Wetjen NM, Marsh WR, Meyer FB, et al. Intracranial electroencephalography seizure onset patterns and surgical outcomes in nonlesional extratemporal epilepsy. *J Neurosurg*. 2009; 110:1147–1152. [PubMed: 19072306]
22. Kerber K, Dumpelmann M, Schelter B, et al. Differentiation of specific ripple patterns helps to identify epileptogenic areas for surgical procedures. *Clin Neurophysiol*. 2014; 125:1339–1345. [PubMed: 24368032]
23. Meltzer JA, Zaveri HP, Goncharova II, et al. Effects of working memory load on oscillatory power in human intracranial EEG. *Cereb Cortex*. 2008; 18:1843–1855. [PubMed: 18056698]
24. Asano E, Nishida M, Fukuda M, et al. Differential visually-induced gamma-oscillations in human cerebral cortex. *NeuroImage*. 2009; 45:477–489. [PubMed: 19135157]
25. Edwards E, Soltani M, Deouell LY, et al. High gamma activity in response to deviant auditory stimuli recorded directly from human cortex. *J Neurophysiol*. 2005; 94:4269–4280. [PubMed: 16093343]

26. Darvas F, Scherer R, Ojemann JG, et al. High gamma mapping using EEG. *NeuroImage*. 2010; 49:930–938. [PubMed: 19715762]
27. Sinai A, Bowers CW, Crainiceanu CM, et al. Electrographic high gamma activity versus electrical cortical stimulation mapping of naming. *Brain*. 2005; 128:1556–1570. [PubMed: 15817517]
28. Melani F, Zelmann R, Mari F, et al. Continuous high frequency activity: a peculiar SEEG pattern related to specific brain regions. *Clin Neurophysiol*. 2013; 124:1507–1516. [PubMed: 23768436]
29. Modur PN, Zhang S, Vitaz TW. Ictal high-frequency oscillations in neocortical epilepsy: implications for seizure localization and surgical resection. *Epilepsia*. 2011; 52:1792–1801. [PubMed: 21762451]
30. Jirsch JD, Urrestarazu E, LeVan P, et al. High-frequency oscillations during human focal seizures. *Brain*. 2006; 129:1593–1608. [PubMed: 16632553]
31. Fujiwara H, Greiner HM, Lee KH, et al. Resection of ictal high-frequency oscillations leads to favorable surgical outcome in pediatric epilepsy. *Epilepsia*. 2012; 53:1607–1617. [PubMed: 22905734]
32. Le Van Quyen M, Bragin A, Staba R, et al. Cell type-specific firing during ripple oscillations in the hippocampal formation of humans. *J Neurosci*. 2008; 28:6104–6110. [PubMed: 18550752]
33. Demont-Guignard S, Benquet P, Gerber U, et al. Distinct hyperexcitability mechanisms underlie fast ripples and epileptic spikes. *Ann Neurol*. 2012; 71:342–352. [PubMed: 22451202]
34. Blanco JA, Stead M, Krieger A, et al. Data mining neocortical high-frequency oscillations in epilepsy and controls. *Brain*. 2011; 134:2948–2959. [PubMed: 21903727]
35. Cho JR, Joo EY, Koo DL, et al. Clinical utility of interictal high-frequency oscillations recorded with subdural macroelectrodes in partial epilepsy. *J Clin Neurol*. 2012; 8:22–34. [PubMed: 22523510]
36. Zaveri HP, Duckrow RB, Spencer SS. On the use of bipolar montages for time-series analysis of intracranial electroencephalograms. *Clin Neurophysiol*. 2006; 117:2102–2108. [PubMed: 16887380]

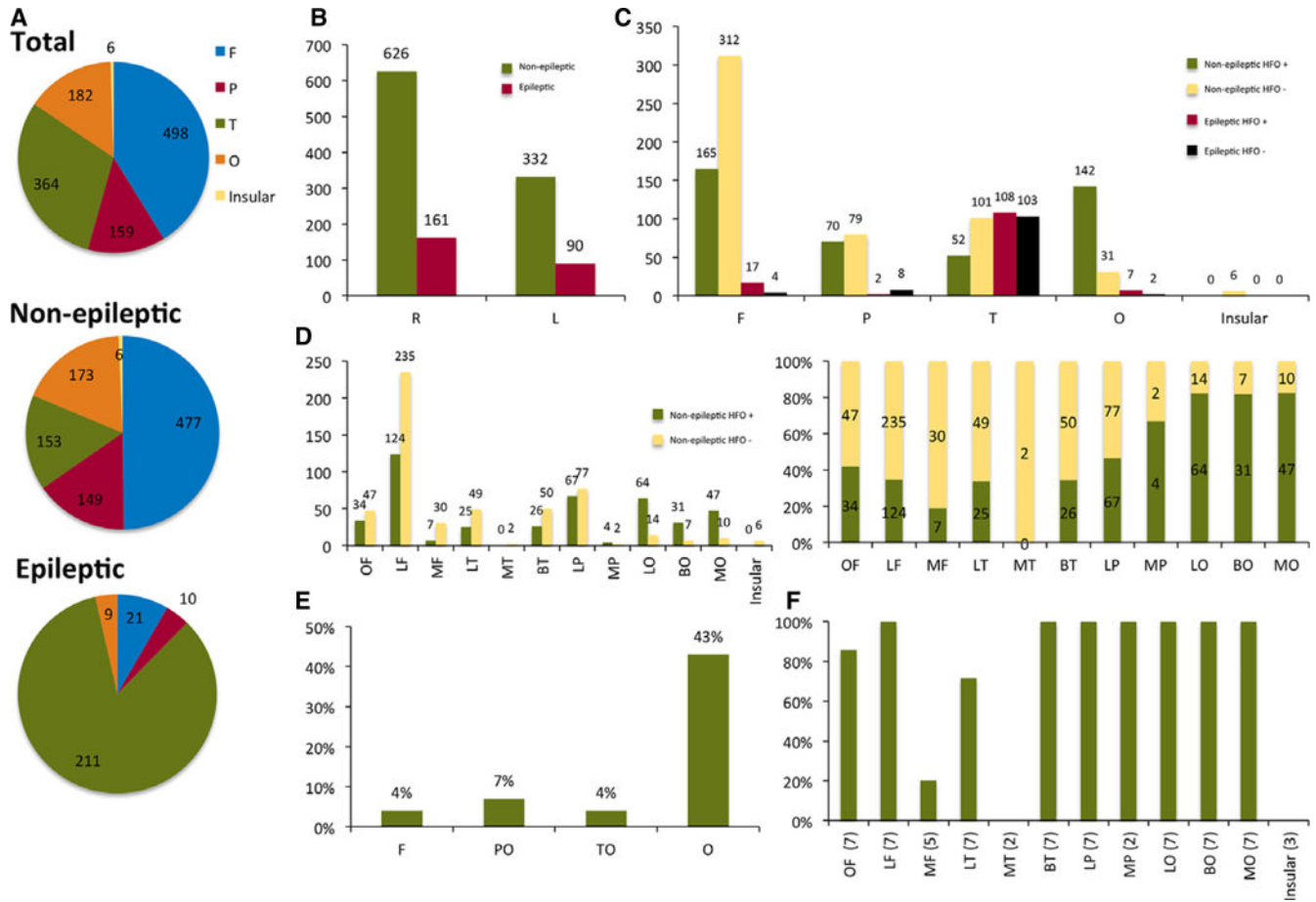


Figure 1. Summary of distribution and classification of contacts in all patients. Numbers represent n of HFO detections unless specified otherwise. **(A)** Lobar localization of all nonepileptic and epileptic contacts. **(B)** Contacts distribution and classification per hemispheres. **(C)** Lobar distribution of contacts and classification according to presence of HFOs and spikes. **(D)** Sublobar distribution of nonepileptic contacts and classification according to presence of HFOs. The right figure represents normalized ratios of nonepileptic contacts with and without HFOs per sublobes. **(E)** Percentage of contacts with high-rate nonepileptic HFOs per lobes. **(F)** Percentage of patients with detected nonepileptic HFOs per region (primarily ripples). Numbers in parentheses denote number of patients with nonepileptic contacts within the region. F, frontal; P, parietal; T, temporal; O, occipital; I, insular; R, right; L, left; OF, orbitofrontal; LF, lateral frontal; MF, mesial frontal; LP, lateral parietal; MP, mesial parietal; BT, basal temporal; LT, lateral temporal; MT, mesial temporal; BO, basal occipital; LO, lateral occipital; MO, mesial occipital; PO, parietooccipital; TO, temporooccipital. *Epilepsia* © ILAE

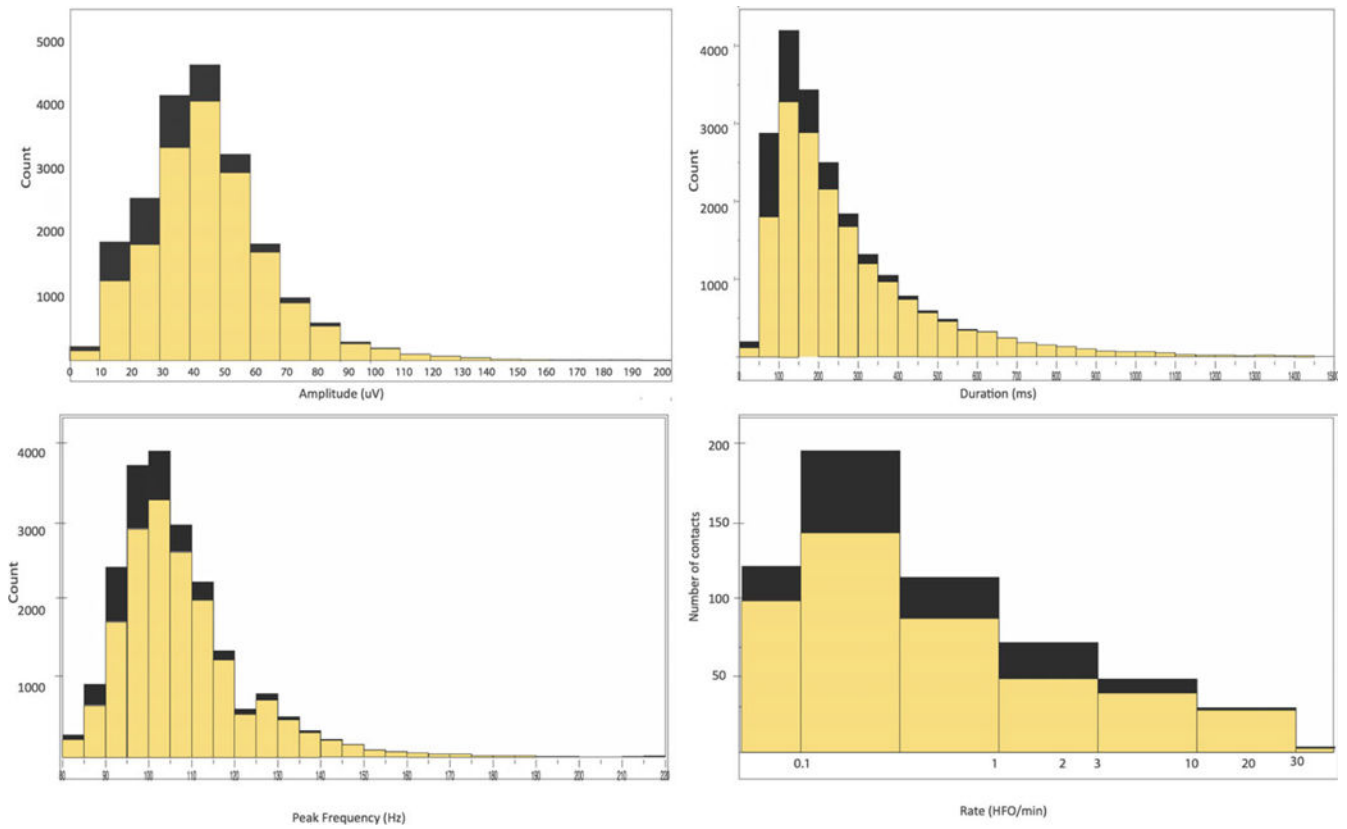


Figure 2. Histograms of amplitude, duration, peak frequency, and rate of nonpileptic (yellow) and pathologic (black) ripples. The x-axis in “ripple rate” is scaled logarithmically.
Epilepsia © ILAE

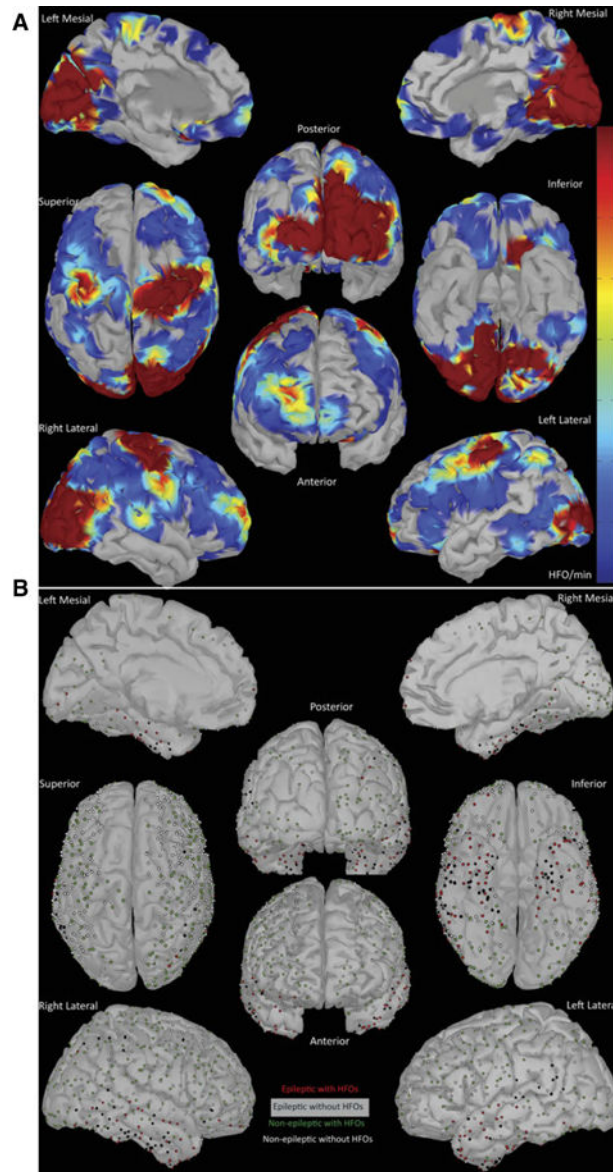
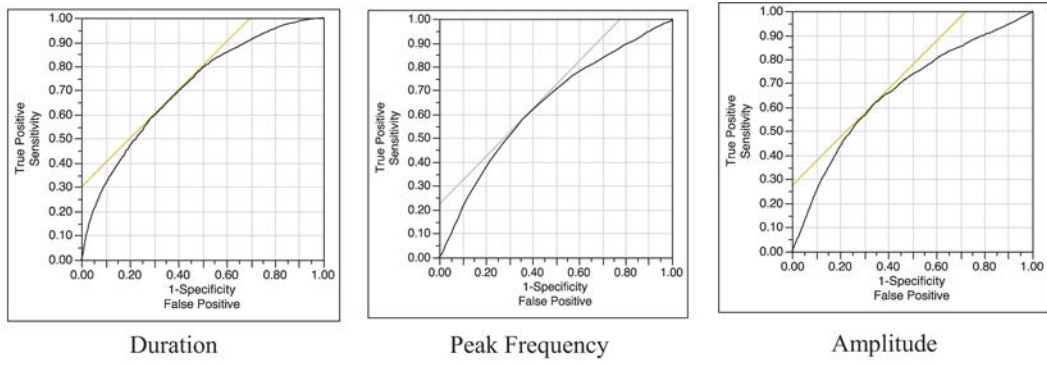


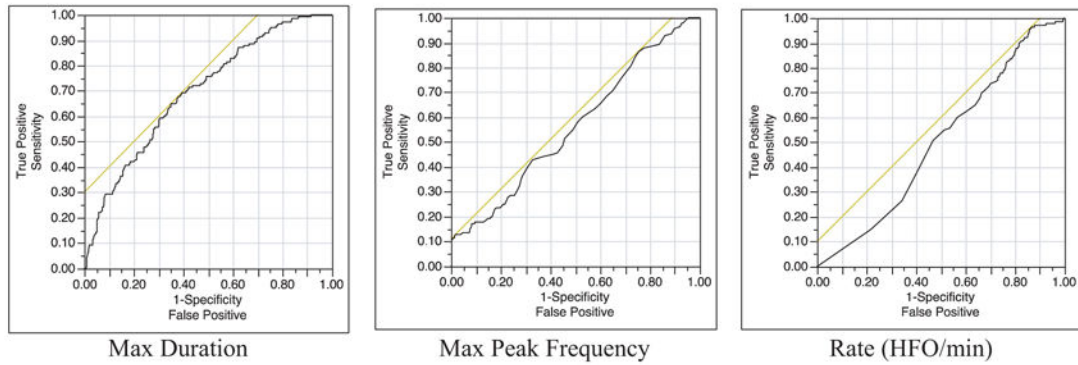
Figure 3.

(A) Distribution of nonepileptic HFOs weighted by rate (HFO event/min, primarily ripples). The rate is projected on a triangular mesh model of a standardized brain. The heat map represents the average rate of HFO events (HFO event/min). We used nearest neighbor linear interpolation in 100 vertices around the center of each electrode contact. Power maps of detected HFOs (not shown) mirror the maps of HFO rates. Areas that were not sampled appear uncolored. (B) Summary of electrode contact placement, classification, and association with HFOs in all the patients. Contact locations are spatially transformed and coregistered with a standardized brain (MNI). The dots mark the location of the centers of the electrodes, and do not represent the size of the electrode. ●, A contact with HFOs in an epileptic site; ●, a contact without HFOs in an epileptic site; ●, a contact with HFOs in a nonepileptic site; ○, a contact without HFOs in a nonepileptic site.

Epilepsia © ILAE



Receiver operating curves and corresponding odds ratios for epileptic vs. nonepileptic at the effective cutoff per HFO event				
	Effective cutoff	AUC	Sen/spec/acc	Odds ratio (p<0.01)
Duration (ms)	<168	.71	.66/.64/.69	3.40 (3.16-3.68)
Amplitude (uV)	<59	.65	.62/.65/.65	3.09(2.87-3.33)
Frequency (HZ)	>100	.64	.58/.64/.63	2.43 (2.26-2.62)



Receiver operating characteristics and corresponding odds ratios for epileptic vs. non-epileptic at the effective cutoff per channel (max value per channel)				
	Effective cutoff	AUC	Sen/spec/acc	Odds ratio (p<0.01)
Duration (ms)	<242	.70	.65/.65/.65	1.78 (1.49-2.13)
Frequency (Hz)	>185	.56	.13/.97/.77	10.00 (3.91-25.92)
Rate (HFO/min)	<4.3	.50	.96/.14/.35	4.22 (1.65 – 10.75)
Amplitude (uV)			Not statistically significant	

$$d = \sqrt{(1 - sensitivity)^2 + (1 - specificity)^2}.$$

Figure 4. Receiver operatic characteristic (ROC) curves per HFO event (ripples) and channels for the following parameters: duration, peak frequency, amplitude, and rate (HFO/min per channel). We used the maximum value within a channel for contact-wise analysis. Odds ratios are applicable on this study’s cohort (i.e. not normalized). The effective cutoffs were calculated to achieve the minimum distance. AUC = Area Under the Curve, Sen = Sensitivity, spec = Specificity, acc = Accuracy.

Epilepsia © ILAE

Author Manuscript

Author Manuscript

Author Manuscript

Author Manuscript

Table 1
Summary of clinical and demographic data, results of presurgical workup, resections, and surgical outcomes

Pt	A/G/H	Onset (years)	Known risk factors	Typical clinical seizure	Sz freq per month	MRI	PET	SPECT (ISAS)	fMRI (language)	Scalp video-EEG	Resection	Follow up (months)	Outcome (Engel)
1	16/M/R	6 (10)	Family history	Gustatory >CPS/auto-motor	80	Decreased R hippocampus size	R temporal	NA	L	R frontotemporal	R anterior temporal	18	Ia
2	20/F/R	11 (9)	AVM/resection	Loud vocalization > "looking spacey"	14	L temporoparietal hemosiderin	NA	NA	R	L temporal	L temporoparietal	17	Ia
3	18/M/R	12 (6)	None	Abdominal aura > CPS > L tonic	4	wnl	R temporal	R temporal + parietal	L	R frontotemporal	R temporal and frontopolar	16	II (1 sz)
4	19/F/R	9 (10)	None	Autonomic + psychic aura > auto-motor	4	Bilateral hippocampus abnormalities	L temporal	L parietal	L	L temporal	None	NA	NA
5	27/F/R	15 (12)	None	Auto-motor > rare second generalization	4	Old R thalamic infarct	R anterior temporal	R temporal	L	R temporoparietal	R temporoparietal	3	Ia
6	10/F/R	5 (5)	Delay	Olfactory > auto-motor/autonomic	150	wnl	L temporal	L temporal	L	L temporal	None	NA	NA
7	49/M/R	28 (21)	Encephalitis	L sensory/auditory auras > GTC	8	R temporal encephalomalacia	R temporal	NA	L	R temporal	R Temporal	3	Ib

Pt, patient; A/G/H, age/gender/handedness; AVM, arteriovenous malformation; Freq, frequency of seizures per month; ISAS, ictal-interictal SPECT analysis by SPM; M, male; F, female; R, right; L, left; CPS, complex partial seizures; wnl, within normal limits; sz, seizure (atypical seizure postoperatively).

Onset (years); numbers in parentheses represent duration of epilepsy in years.